

This is the accepted manuscript made available via CHORUS. The article has been published as:

## Multiple Charge Density Waves and Superconductivity Nucleation at Antiphase Domain Walls in the Nematic Pnictide $\text{Ba}_{1-x}\text{Sr}_x\text{Ni}_2\text{As}_2$

xmlns="http://www.w3.org/1998/Math/MathML" display="inline">
$$\text{Ba}_{1-x}\text{Sr}_x\text{Ni}_2\text{As}_2$$

Sangjun Lee, John Collini, Stella X.-L. Sun, Matteo Mitrano, Xuefei Guo, Chris Eckberg, Johnpierre Paglione, Eduardo Fradkin, and Peter Abbamonte

Phys. Rev. Lett. **127**, 027602 — Published 6 July 2021

DOI: [10.1103/PhysRevLett.127.027602](https://doi.org/10.1103/PhysRevLett.127.027602)

# Multiple charge density waves and superconductivity nucleation at antiphase domain walls in the nematic pnictide $\text{Ba}_{1-x}\text{Sr}_x\text{Ni}_2\text{As}_2$

Sangjun Lee,<sup>1</sup> John Collini,<sup>2</sup> Stella X.-L. Sun,<sup>1</sup> Matteo Mitrano,<sup>1</sup> Xuefei Guo,<sup>1</sup> Chris Eckberg,<sup>2</sup> Johnpierre Paglione,<sup>2,3</sup> Eduardo Fradkin,<sup>1,4</sup> and Peter Abbamonte<sup>1,\*</sup>

<sup>1</sup>*Department of Physics and Materials Research Laboratory,  
University of Illinois, Urbana, Illinois 61801, USA*

<sup>2</sup>*Maryland Quantum Materials Center, Department of Physics,  
University of Maryland, College Park, Maryland 20742, USA*

<sup>3</sup>*Canadian Institute for Advanced Research, Toronto, ON M5G 1Z8, Canada*

<sup>4</sup>*Institute of Condensed Matter Theory, University of Illinois, Urbana, Illinois 61801, USA*

How superconductivity interacts with charge or nematic order is one of the great unresolved issues at the center of research in quantum materials.  $\text{Ba}_{1-x}\text{Sr}_x\text{Ni}_2\text{As}_2$  (BSNA) is a charge ordered pnictide superconductor recently shown to exhibit a six-fold enhancement of superconductivity due to nematic fluctuations near a quantum phase transition (at  $x_c = 0.7$ ) [1]. The superconductivity is, however, anomalous, with the resistive transition for  $0.4 < x < x_c$  occurring at a higher temperature than the specific heat anomaly. Using x-ray scattering, we discovered a new charge density wave (CDW) in BSNA in this composition range. The CDW is commensurate with a period of two lattice parameters, and is distinct from the two CDWs previously reported in this material [1, 2]. We argue that the anomalous transport behavior arises from heterogeneous superconductivity nucleating at antiphase domain walls in this CDW. We also present new data on the incommensurate CDW, previously identified as being unidirectional [2], showing that it is a rotationally symmetric, “ $4Q$ ” state with  $C_4$  symmetry. Our study establishes BSNA as a rare material containing three distinct CDWs, and an exciting testbed for studying coupling between CDW, nematic, and SC orders.

One of the perennial questions in quantum materials is to what extent superconductivity (SC) may be enhanced by coupling to other Fermi surface instabilities, such as charge density wave (CDW), spin density wave (SDW) or nematic orders. This issue has been investigated most widely in cuprate and iron-based superconductors [3–6]. While spin fluctuations are considered a primary ingredient in Cooper pairing in both materials, the CDW in cuprates [7–9] and nematic fluctuations in iron-based materials [10, 11] are pervasive and suggest a close interrelation between SC and these other electronic instabilities. The importance of such orderings for SC is still unclear, so there is a great need for new materials that can provide fresh insight.

$\text{Ba}_{1-x}\text{Sr}_x\text{Ni}_2\text{As}_2$  is a nickel-based pnictide superconductor that is an ideal system to investigate the relationship between charge instabilities and SC. We recently showed that  $\text{BaNi}_2\text{As}_2$  exhibits two distinct CDW instabilities that arise sequentially on lowering temperature [2]. In the tetragonal phase, an incommensurate CDW (IC-CDW), previously identified as unidirectional, forms along the in-plane  $H$  axis with wave vector  $q = 0.28$ . Upon cooling across the structural transition to triclinic phase, the IC-CDW is replaced by the second CDW, which we denote C-CDW-1, that is commensurate with  $q = 1/3$ . This CDW arises via a lock-in transition from an incipient, slightly incommensurate CDW with  $q \sim 0.31$  [2].

When  $\text{BaNi}_2\text{As}_2$  is substituted with Sr or Co, the triclinic phase that hosts C-CDW-1 is suppressed and a SC dome emerges [1, 2, 12], suggesting C-CDW-1 plays a similar role to antiferromagnetism in chemically-substituted  $\text{BaFe}_2\text{As}_2$ . Further, full suppression of the

CDW by Sr substitution, which occurs at the critical composition  $x_c = 0.7$ , results in a quantum phase transition (QPT) characterized by nematic fluctuations that drive a sixfold enhancement of the superconducting  $T_c$  [1, 13].  $\text{Ba}_{1-x}\text{Sr}_x\text{Ni}_2\text{As}_2$  is therefore an exciting new system in which the interaction between SC, CDW, and nematic order can be studied in detail.

Recent studies revealed two peculiar properties of  $\text{Ba}_{1-x}\text{Sr}_x\text{Ni}_2\text{As}_2$  that are not fully understood [1, 2]. First, for the composition range of  $0.4 < x < x_c$ , the SC transition in transport measurements is broadened and occurs at a higher temperature than the specific heat anomaly [1]. Why the resistive and thermodynamic transitions should be split in this manner is not known. Second, the IC-CDW was identified in Ref. [1] as a lattice-driven instability, without electronic character, since it shows no precursor response in the nematic susceptibility. However, it was also observed that the elastoresistance becomes hysteretic whenever the IC-CDW is present, suggesting the two phases are coupled. These two observations are seemingly contradictory, since a purely structural phase transition should not influence the nematic response in this way. The nature of the interaction between the IC-CDW and the nematic phase remains unclear.

Here, using x-ray scattering, we present the discovery of a *third* CDW in  $\text{Ba}_{1-x}\text{Sr}_x\text{Ni}_2\text{As}_2$ , which we denote C-CDW-2, in the composition range  $0.4 < x < x_c$ , where  $x_c = 0.7$ . This CDW is commensurate with a period of two lattice parameters (period-2). While a CDW with a generic wave vector has a complex order parameter [14], the period-2 CDW state is special in that its order parameter is real. We will show below that competing (weaker)

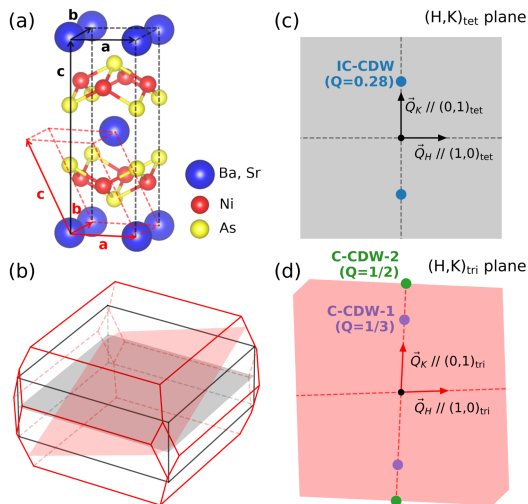


FIG. 1. (a) The crystal structure of  $\text{Ba}_{1-x}\text{Sr}_x\text{Ni}_2\text{As}_2$  and the unit cells of tetragonal (black lines) and triclinic phases (red lines). (b) The BZ boundaries of tetragonal (black lines) and triclinic (red lines) phases. The planes colored in black and red represent  $H$ - $K$  planes in the tetragonal and triclinic phases, respectively. (c), (d) The  $H$ - $K$  planes of tetragonal and triclinic phases, respectively, showing the location of three CDWs in momentum space in each phase.

SC state can be nucleated on topological defects of a period-2 CDW such as domain walls. The implication is that the phase at  $0.4 < x < x_c$  may be a heterogeneous state in which SC resides at the topological defects of the CDW order.

Further, we report a wider x-ray momentum survey showing that the IC-CDW phase is in fact bidirectional with  $90^\circ$  rotational symmetry. We observed additional satellite reflections demonstrating a coherent “ $4Q$ ” state with  $C_4$  symmetry that does not break the rotational symmetry of the underlying tetragonal lattice. This observation explains the absence of a precursor nematic response in elastoresistivity measurements [1], and suggests this CDW could be electronic and strongly coupled to the nematic order.

Single crystals of  $\text{Ba}_{1-x}\text{Sr}_x\text{Ni}_2\text{As}_2$  with  $x = 0, 0.27, 0.42, 0.47, 0.65,$  and  $0.73$  were measured in this study. Three-dimensional x-ray surveys of momentum space were obtained using a Mo  $K_\alpha$  (17.4 keV) microspot x-ray source and a Mar345 image plate detector by sweeping crystals through an angular range of  $20^\circ$ . All temperature evolution measurements in this study are conducted while warming the samples starting from low temperature (see Supplemental Material (SM) for experimental details [15]).

The parent compound,  $\text{BaNi}_2\text{As}_2$ , has tetragonal  $I4/mmm$  symmetry at room temperature and undergoes a phase transition to triclinic  $P\bar{1}$  at  $T_s = 136$  K [2, 16]. This transition is observed in x-ray measurements as a splitting of the tetragonal reflections into four peaks due to the formation of triclinic twin domains [2, 16] (see

SM for more details [15]). Measurements in the triclinic phase were indexed by selecting a single subset of these four reflections, emphasizing scattering from a single domain. Figures 1(a) and (b) show the conventional unit cells and the BZ boundaries in the tetragonal and triclinic phases. Throughout this letter, we use  $(H, K, L)_{\text{tet}}$  and  $(H, K, L)_{\text{tri}}$  to denote indices in the tetragonal and triclinic unit cells, respectively.

Here, we find that when  $\text{BaNi}_2\text{As}_2$  is substituted with Sr, the triclinic transition as seen with x-rays initially increases in temperature, reaching a maximum  $T_s = 141$  K at  $x = 0.27$ . Further substitution decreases  $T_s$  until, at  $x = 0.73$ , the structure transition is no longer observed, indicating a quantum phase transition at  $x_c \sim 0.7$ , consistent with conclusions from transport experiments [1]. In Fig. 5 we compare our results to the transport phase diagram of  $\text{Ba}_{1-x}\text{Sr}_x\text{Ni}_2\text{As}_2$ . The triclinic transition determined by x-ray scattering while warming (purple line) is slightly higher in temperature than the cooling transition determined by transport (black dashed line) [1], demonstrating the first order nature of the transition. Nevertheless, we see no evidence for coexistence of tetragonal and triclinic phases, unlike Co-substituted compounds,  $\text{Ba}(\text{Ni}_{1-x}\text{Co}_x)_2\text{As}_2$ , in which an extended region of coexistence occurs [2].

The primary result of this study is the discovery in the composition range  $0.4 < x < x_c$  of a third CDW, which we denote C-CDW-2. This CDW is distinct from the IC-CDW and C-CDW-1 phases reported previously [1, 2]. Figure 2 shows x-ray measurements of the sample with  $x = 0.42$ , in which all three CDWs are observed sequentially upon cooling. The IC-CDW forms at the highest temperature, at  $T_{1C} = 132.5 \pm 2.5$  K. Its wave vector, shown in the (1,1,5) BZ in Figs. 2(a),(d), is  $q = (0, 0.28, 0)_{\text{tet}}$ , which is the same reported in the parent compound [2]. No corresponding reflection was observed at  $(0.28, 0, 0)_{\text{tet}}$  in this zone, which previously led us to the conclusion that the IC-CDW is unidirectional [2]. Below, we present data revising this conclusion. In Co-substituted materials, the IC-CDW was only observed in the parent compound and disappeared at Co content of 0.07 [2]. We note that the IC-CDW could be present at intermediate Co substitution in  $\text{Ba}(\text{Ni}_{1-x}\text{Co}_x)_2\text{As}_2$ , just as it persists up to  $x = 0.47$  in  $\text{Ba}_{1-x}\text{Sr}_x\text{Ni}_2\text{As}_2$ .

Upon further cooling, the IC-CDW is replaced by C-CDW-1 at  $T_{C1} = 117.5 \pm 2.5$  K [Figs. 2(b),(e)], which coincides with the triclinic transition. Its wave vector is  $q = (0, 1/3, 0)_{\text{tri}}$ , which is commensurate with a period of three lattice parameters. As in the case of IC-CDW, no  $(1/3, 0, 0)_{\text{tri}}$  peak was observed. This CDW is also observed in Co-substituted compounds, where it exhibits a lock-in effect [2]. However, we observe no lock-in effect in Sr-substituted materials.

A third, previously unobserved CDW, which we call C-CDW-2, appears at lower temperature,  $T_{C2} = 95 \pm 5$  K [Figs. 2(c),(f)]. Its wave vector,  $q = (0, 1/2, 0)_{\text{tri}}$

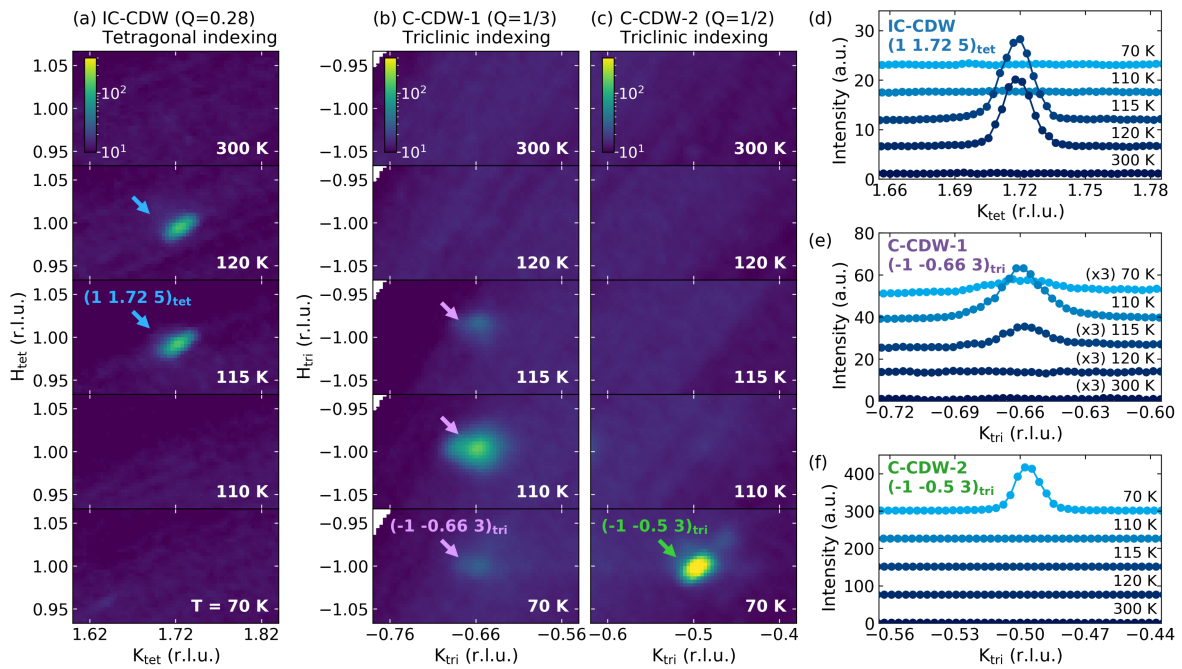


FIG. 2. Three distinct CDWs in  $\text{Ba}_{0.58}\text{Sr}_{0.42}\text{Ni}_2\text{As}_2$ . (a), (b), (c)  $H$ - $K$  maps of IC-CDW, C-CDW-1, and C-CDW-2, respectively, at a selection of temperatures. (d), (e), (f) Line momentum scans of the CDW reflections shown in (a), (b), and (c), respectively, along the corresponding modulation direction.

is commensurate with a period of two lattice parameters. Again, no corresponding peak was observed at  $q = (1/2, 0, 0)_{\text{tri}}$ . When C-CDW-2 forms, the magnitude of the triclinic distortion increases [Fig. S1(c) in SM [15]] while the C-CDW-1 order parameter is suppressed [Fig. 4(c)]. This indicates that C-CDW-2 competes with C-CDW-1, but has a cooperative relationship with the triclinic phase itself. None of these effects were observed in  $\text{Ba}(\text{Ni}_{1-x}\text{Co}_x)_2\text{As}_2$ , indicating that C-CDW-2 is specific to the current material and does not arise with Co substitution. We summarize the momentum space locations of all three CDWs in Fig. 1(b)-(d). We emphasize that these three CDWs reside in very different locations in momentum space, as illustrated in Fig. 1; the difference between the three CDW wave vectors is not merely due to a change of indexing coordinates.

We now discuss the rotational symmetry of the three CDWs. The satellite reflections in all three phases appear in only one direction in a given BZ, which would normally be interpreted as evidence that all three CDWs are unidirectional. This is unsurprising for C-CDW-1 and C-CDW-2 since they reside in the triclinic phase in which  $C_4$  (rotational) symmetry is broken by the underlying lattice. However, it is puzzling that IC-CDW should also be unidirectional, since it resides in the tetragonal phase where  $C_4$  symmetry is preserved. Our claim that IC-CDW is unidirectional [2] led the authors of Ref. [1] to conclude that the IC-CDW is a purely structural phase transition, uncoupled to the valence electron system, since they observed no precursor response in the ne-

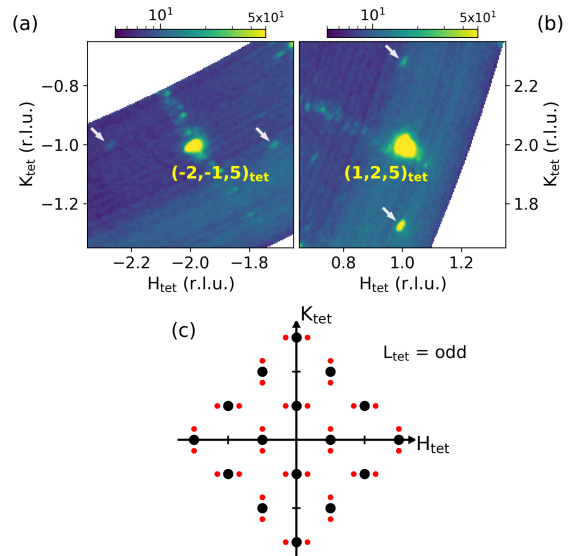


FIG. 3. (a)  $H$ - $K$  map around  $(-2, -1, 5)_{\text{tet}}$  showing the IC-CDW satellites at  $(\pm 0.28, 0, 0)_{\text{tet}}$ . The satellites are absent at  $(0, \pm 0.28, 0)_{\text{tet}}$ . (b)  $H$ - $K$  map around  $(1, 2, 5)_{\text{tet}}$  showing the satellites at  $(0, \pm 0.28, 0)_{\text{tet}}$ . The satellites are absent at  $(\pm 0.28, 0, 0)_{\text{tet}}$ . (c) Illustration of the symmetry pattern of IC-CDW in  $H$ - $K$  plane at odd-numbered  $L$ . Black dots represent Bragg peak locations, and red dots represent IC-CDW peak locations.

matic susceptibility expected of an electronic phase with broken rotational symmetry.

We reexamined this issue by performing a wide, three-

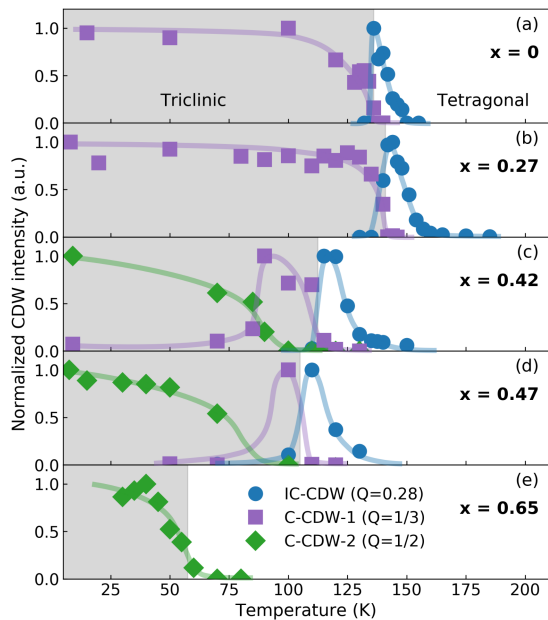


FIG. 4. Warming temperature dependence of the integrated intensities of the IC-CDW (blue circles), C-CDW-1 (purple squares), and C-CDW-2 (green diamonds) reflections. The Sr composition,  $x$ , is shown in each panel. The shaded region represents the temperature range of the triclinic phase. Each curve is scaled to the maximum CDW intensity at low temperature. The solid lines are guides to the eye.

dimensional x-ray survey of a  $20^\circ$  wedge of momentum space, analyzing where CDW satellites reside in multiple BZs. We found that the C-CDW-1 and C-CDW-2 show the same unidirectionality in all zones observed (see SM [15]), affirming that these triclinic CDWs are unidirectional as claimed [2]. However, the IC-CDW exhibits the more complicated pattern shown in Fig. 3. While any given BZ has only two satellites, their orientation is different in different BZs. The overall pattern is invariant under  $90^\circ$  rotations around the origin, and therefore exhibits the same  $C_4$  symmetry as the underlying tetragonal lattice. We conclude that the IC-CDW is not unidirectional, but is a coherent “ $4Q$ ” state in which two reflections in each BZ are extinguished by some additional symmetry. This result implies that IC-CDW may be electronic in origin after all, and may couple strongly to the nematic order.

Figure 4 summarizes the behavior of the three CDWs over the full range of Sr composition investigated. The IC-CDW is present from  $x = 0$  to 0.47. The C-CDW-2 phase is first observed at  $x = 0.42$ , where it replaces C-CDW-1 in the triclinic phase, and persists up to  $x = 0.65$  [17]. At  $x = 0.73$ , no CDW transition is observed. No two CDWs are ever optimized at the same composition or temperature, indicating that the three phases likely compete with one another.

A summary phase diagram of  $\text{Ba}_{1-x}\text{Sr}_x\text{Ni}_2\text{As}_2$  is presented in Fig. 5. The anomalous superconducting phase at  $0.4 < x < x_c$ , in which transport and thermodynamic

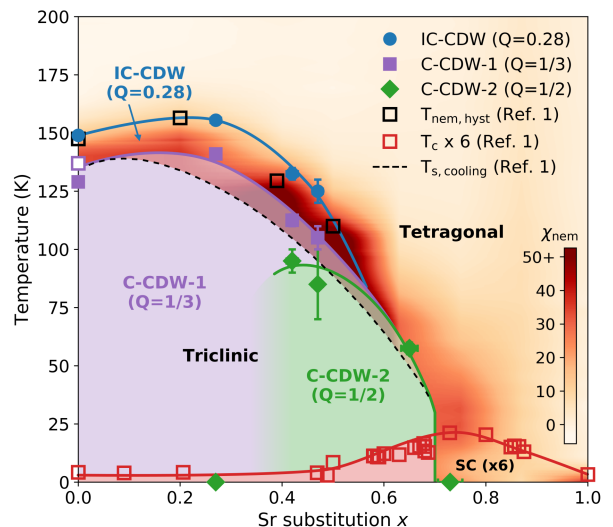


FIG. 5. Phase diagram of  $\text{Ba}_{1-x}\text{Sr}_x\text{Ni}_2\text{As}_2$  showing the IC-CDW (blue circles), C-CDW-1 (purple squares), C-CDW-2 (green diamonds) phases. The hollow purple square at  $x = 0$  represents the onset of the incipient CDW that undergoes a lock-in transition and evolves to C-CDW-1. The triclinic phase boundary on warming coincides with the boundary of C-CDW-1 and C-CDW-2. The overlaid color scale represents the nematic susceptibility,  $\chi_{\text{nem}}$ . The onset of the strain-hysteresis of the nematic response,  $T_{\text{nem,hyst}}$  (black hollow squares), and the resistive superconducting  $T_c$  (red hollow squares) are shown together for comparison.

signatures occur at different temperatures [1], resides entirely within the C-CDW-2 phase. By contrast, at  $x > x_c$  when no CDW is present, the superconducting signatures are normal. This implies that the peculiar superconducting state reported in Ref. [1] is connected to the presence of C-CDW-2.

A period-2 CDW competing with superconductivity is prone to developing a heterogeneous mixed state. The order parameter of period-2 CDW is real, since its phase can only be either 0 or  $\pi$ , i.e., the order parameter itself is either  $\psi$  or  $-\psi$  where  $\psi$  is a real number [15]. A CDW is highly sensitive to disorder [18], trace amounts of which can lead to the formation of domain walls with a  $\pi$  phase shift, across which the order parameter changes sign and, thus, vanishes. Since the CDW is suppressed at the domain walls, these locations are favorable for competing superconductivity to emerge, resulting in a heterogeneous or filamentary superconducting state. In SM Sec. VI [15], we present a quantitative theory of this situation. We consider the simplest form of the Landau-Ginzburg free energy with competing CDW and SC orders as given by Eq. (2) in SM, and obtain solutions in the presence of a domain wall. The corresponding Landau-Ginzburg equation [Eq. (12) in SM] has a non-trivial domain wall solution in which the CDW order parameter changes sign. At the location of the topological defect, the SC order parameter is nonzero, and decays exponentially away from the domain wall. We therefore

identify this unusual SC state as a heterogeneous state in which SC is locally formed at domain walls of C-CDW-2 that are consequence of any disorder present in the system. A system with a finite density of such defects would exhibit a thermodynamic transition to a uniform SC phase driven by Josephson coupling among nearby domain walls, albeit with a highly-reduced  $T_c$  [19]. Thus, the onset of the resistive transition is where the CDW domain walls become superconducting, with macroscopic superconductivity being achieved at lower temperatures.

Another feature of the phase diagram (Fig. 5) is that there is a close correspondence between the presence of the IC-CDW and irreversible behavior in the nematic susceptibility measured with elastoresistance techniques [1]. When the IC-CDW is present, the strain response is hysteretic. As discussed above, it is possible that the IC-CDW couples strongly to the nematic order parameter, and therefore pins the nematic fluctuations. The hysteretic response then can be understood as the training of these static nematic domains by the applied elastic strain field. When the IC-CDW is absent, the nematic domains become dynamic, the response becomes reversible, and the fluctuations enhance superconductivity near  $x_c = 0.7$ , as claimed in Ref. [1].

Recently, Merz et al. [20] reported that  $\text{BaNi}_2\text{As}_2$  is, in fact, orthorhombic in the IC-CDW phase. We see no evidence for such orthorhombicity in our study, though the magnitude of the orthorhombic distortion reported in Ref. [20] would be below our detection limit. The existence of such a phase could require a reinterpretation of the symmetry pattern of IC-CDW [Fig. 3(c)]. More detailed refinements of the crystal structure would shed light on this issue.

In summary, we showed that  $\text{Ba}_{1-x}\text{Sr}_x\text{Ni}_2\text{As}_2$  exhibits three distinct charge density waves, IC-CDW, C-CDW-1 and C-CDW-2. The order parameter of C-CDW-2, which is period-2, is always zero at antiphase domain walls, allowing the competing superconductivity to emerge locally. We also showed that the IC-CDW can strongly couple to the nematic order parameter, and promote static nematic domains by pinning the fluctuations. Our study establishes BSNA as a rare example of a material containing three distinct CDWs, and an exciting testbed for studying coupling between CDW, nematic, and SC orders.

We thank P. Ghaemi for an early collaboration, and S. A. Kivelson for discussions. X-ray experiments were supported by the U.S. Department of Energy, Office of Basic Energy Sciences grant no. DE-FG02-06ER46285 (PA). Theory work was supported in part by the U.S. National Science Foundation grant DMR 1725401 (EF). Materials synthesis was supported by the National Science Foundation Grant no. DMR1905891 (JP). P. A. and J. P. acknowledge the Gordon and Betty Moore Foundations EPIQS Initiative through grant nos. GBMF9452 and GBMF9071, respectively.

- \* [abbamonte@mrl.illinois.edu](mailto:abbamonte@mrl.illinois.edu)
- [1] C. Eckberg, D. J. Campbell, T. Metz, J. Collini, H. Hodovanets, T. Drye, P. Zavalij, M. H. Christensen, R. M. Fernandes, S. Lee, P. Abbamonte, J. W. Lynn, and J. Paglione, *Nature Physics* **16**, 346 (2020).
  - [2] S. Lee, G. de la Peña, S. X.-L. Sun, M. Mitrano, Y. Fang, H. Jang, J.-S. Lee, C. Eckberg, D. Campbell, J. Collini, J. Paglione, F. M. F. de Groot, and P. Abbamonte, *Phys. Rev. Lett.* **122**, 147601 (2019).
  - [3] E. Fradkin, S. A. Kivelson, and J. M. Tranquada, *Rev. Mod. Phys.* **87**, 457 (2015).
  - [4] J. M. Tranquada, *Physica B: Condensed Matter* **460**, 136 (2015).
  - [5] J. Paglione and R. L. Greene, *Nat. Phys.* **6**, 645 (2010).
  - [6] P. Dai, *Rev. Mod. Phys.* **87**, 855 (2015).
  - [7] P. Abbamonte, A. Rusydi, S. Smadici, G. D. Gu, G. A. Sawatzky, and D. L. Feng, *Nature Physics* **1**, 155 (2005).
  - [8] G. Ghiringhelli, M. Le Tacon, M. Minola, S. Blanco-Canosa, C. Mazzoli, N. B. Brookes, G. M. De Luca, A. Frano, D. G. Hawthorn, F. He, T. Loew, M. M. Sala, D. C. Peets, M. Salluzzo, E. Schierle, R. Sutarto, G. A. Sawatzky, E. Weschke, B. Keimer, and L. Braicovich, *Science* **337**, 821 (2012).
  - [9] R. Comin and A. Damascelli, *Annual Review of Condensed Matter Physics* **7**, 369 (2016).
  - [10] J.-H. Chu, H.-H. Kuo, J. G. Analytis, and I. R. Fisher, *Science* **337**, 710 (2012).
  - [11] H.-H. Kuo, J.-H. Chu, J. C. Palmstrom, S. A. Kivelson, and I. R. Fisher, *Science* **352**, 958 (2016).
  - [12] C. Eckberg, L. Wang, H. Hodovanets, H. Kim, D. J. Campbell, P. Zavalij, P. Piccoli, and J. Paglione, *Phys. Rev. B* **97**, 224505 (2018).
  - [13] S. Lederer, E. Berg, and E.-A. Kim, *Phys. Rev. Res.* **2**, 023122 (2020).
  - [14] W. L. McMillan, *Phys. Rev. B* **12**, 1187 (1975).
  - [15] See Supplemental Material [URL will be inserted by publisher] for the experimental details, the lattice parameters of samples and structural transitions, the symmetry patterns of CDWs, and for details of the theory, which includes Refs. [21-30].
  - [16] A. S. Sefat, M. A. McGuire, R. Jin, B. C. Sales, D. Mandrus, F. Ronning, E. D. Bauer, and Y. Mozharivskyj, *Phys. Rev. B* **79**, 094508 (2009).
  - [17] J. Collini, et al., to be published.
  - [18] Y. Imry and S.-K. Ma, *Phys. Rev. Lett.* **35**, 1399 (1975).
  - [19] V. J. Emery, E. Fradkin, S. A. Kivelson, and T. C. Lubensky, *Phys. Rev. Lett.* **85**, 2160 (2000).
  - [20] M. Merz, L. Wang, T. Wolf, P. Nagel, C. Meingast, and S. Schuppler, [arXiv:2012.05024](https://arxiv.org/abs/2012.05024).
  - [21] C. Chen, L. Su, A. H. Castro Neto, and V. M. Pereira, *Phys. Rev. B* **99**, 121108 (2019).
  - [22] W. L. McMillan, *Phys. Rev. B* **14**, 1496 (1976).
  - [23] T. Nattermann, in *Spin Glasses and Random Fields* (World Scientific, Singapore, 1998) pp. 277–298, [arXiv:cond-mat/9705295](https://arxiv.org/abs/cond-mat/9705295).
  - [24] L. D. Landau and E. M. Lifshitz, *Quantum Mechanics: Non-Relativistic Theory*, Course of Theoretical Physics, Vol. v.3 (Butterworth-Heinemann, Oxford, 1991).
  - [25] Y. I. Joe, X. M. Chen, P. Ghaemi, K. D. Finkelstein, G. A. de la Peña, Y. Gan, J. C. T. Lee, S. Yuan, J. Geck, G. J. MacDougall, T. C. Chiang, S. L. Cooper, E. Fradkin, and P. Abbamonte, *Nature Physics* **10**, 421 (2014).

- [26] J. E. Hoffman, E. W. Hudson, K. M. Lang, V. Madhavan, H. Eisaki, S. Uchida, and J. C. Davis, *Science* **295**, 466 (2002).
- [27] S. A. Kivelson, D.-H. Lee, E. Fradkin, and V. Oganesyan, *Phys. Rev. B* **66**, 144516 (2002).
- [28] Y. Yu and S. A. Kivelson, *Phys. Rev. B* **99**, 144513 (2019).
- [29] B. Kalisky, J. R. Kirtley, J. G. Analytis, J.-H. Chu, A. Vailionis, I. R. Fisher, and K. A. Moler, *Phys. Rev. B* **81**, 184513 (2010).
- [30] H. Xiao, T. Hu, A. P. Dioguardi, N. apRoberts Warren, A. C. Shockley, J. Crocker, D. M. Nisson, Z. Viskadourakis, X. Tee, I. Radulov, C. C. Almasan, N. J. Curro, and C. Panagopoulos, *Phys. Rev. B* **85**, 024530 (2012).